Available online at www.sciencedirect.com
ScienceDirect
Coordination Chemistry Reviews 253 (2009) 21–36
COORDINATION CHEMISTRY REVIEWS
www.elsevier.com/locate/ccr

Review

Ferrocene-appended porphyrins: Syntheses and properties

Christophe Bucher*, Charles H. Devillers, Jean-Claude Moutet, Guy Royal, Eric Saint-Aman

Université Joseph Fourier, Département de Chimie Moléculaire (UMR CNRS/UJF 5250), Laboratoire de Chimie Inorganique Rédox, BP-53, 38041 Grenoble Cedex 9, France

Received 24 September 2007; accepted 24 November 2007
Available online 4 December 2007

Contents

Abstract

This review article focuses on the syntheses and potential applications of ferrocene-appended porphyrin architectures. Several strategies have been developed to date to associate ferrocenyl fragments and porphyrin rings in the same molecular architecture, depending on the targeted application: (i) connection at a *meso* position through a direct linkage, a conjugated or saturated spacer or using a non-covalent approach and (ii) connection at a β-pyrrolic position. Examples of ferrocene–porphyrin analogues are also presented.

Keywords: Ferrocene; Porphyrins

1. Introduction

Ferrocene and porphyrins have already been associated following various strategies and with quite different objectives. Their donor–acceptor complementary and their electrochemical activities have especially been exploited to investigate photoinduced electron transfer processes and to mimic photosynthesis active sites [1,2]. Their multiple redox active centres are also of fundamental importance for the development of molecular-based electronic devices [3,4] or molecular electrogenic sensors [5]. Their ability to reversibly accept and/or release several electrons at distinct potentials is particularly interesting in multi-electron redox catalysis [6] and can be used for multibit information storage at the molecular level [7,8]. The porphyrin substitution pattern and the nature of the organic linkage between these redox active centres have also been shown to drastically influence their "communication" and numerous studies aimed at characterizing and understanding these interactions. Due to its unique structural and electronic properties, combined with an extensive chemical reactivity, the redox responsive unit ferrocene has been without doubt the most widely associated metallocene and there are only few examples of porphyrins linked to non-iron containing metallocenes or related organometallic fragments [9–14]. A large variety of ferrocene-appended porphyrins or porphyrin analogues can be found in the literature and we choose to review these structures as a function of their association mode which has been achieved directly or through various

* Corresponding author. Tel.: +33 4 76 51 46 82; fax: +33 4 76 51 42 67.
E-mail address: christophe.bucher@ujf-grenoble.fr (C. Bucher).

0010-8545/$ – see front matter © 2007 Elsevier B.V. All rights reserved.
doi:10.1016/j.ccr.2007.11.025

spacers linked to the *meso*- or β-pyrrolic positions of porphyrins.

2. *Meso*-linked ferrocene–porphyrins

2.1. Direct connection

The first example of direct linkage between a porphyrin and a ferrocenyl subunit was reported by Wollmann and Hendrickson [15] upon reacting ferrocene–carboxaldehyde with pyrrole in refluxing propionic acid (Fig. 1, path A). After purification of the crude mixture, this Alder and Longo-like [16] procedure yielded the targeted 5,10,15,20-tetrakis(ferrocenyl)porphyrin $\mathbf{1}H_2$ in 40% yield.

The authors attributed the unusual broadness of the signals observed in the ^{1}H NMR spectrum of the latter to the existence of inseparable atropoisomers which are defined by the relative orientation of the bulky ferrocenyl groups with respect to the planar porphyrin macrocycle. However, the spectroscopic features of this species turned out to be significantly different from those of the same molecule isolated 20 years latter by Loim et al. [12] in 40% yield using a milder Lindsey-like [19,20] procedure (Fig. 1, path B), upon condensing ferrocene–carboxaldehyde with pyrrole in the presence of a Lewis acid followed by oxidation with *p*-chloranil (TCQ), or more recently synthesized by Chandrashekar and co-workers [17,18] according to a similar procedure starting from a ferrocenyl-dipyrromethane (Fig. 1, path C). The significant discrepancies between the ^{1}H NMR and UV–vis spectroscopic signatures reported for $\mathbf{1}H_2$ led several authors to question the nature of the original species isolated by Wollmann and Hendrickson under rather hard experimental conditions (refluxing in propionic acid).

The physico-chemical properties of the free base $\mathbf{1}H_2$ bearing four bulky ferrocenyl derivatives were investigated by several groups. Its photochemical and photophysical properties were studied by Nadtochenko et al. [21,22] who demonstrated the ferrocene-based quenching of the porphyrin fluorescence and showed that the fluorescence quantum yield of $\mathbf{1}H_2$ is highly altered by the ferrocene groups, estimating that it is 10^5 times lower than that of the 5,10,15,20-tetrakis(phenyl)porphyrin ($TPPH_2$). The relaxation of the Q1(π–π*) excited state of $\mathbf{1}H_2$ and its diprotonated form $\mathbf{1}H_4^{2+}$ was also investigated by femtosecond laser absorption spectroscopy: the transition to the charge transfer state was shown to occur within 208 ± 10 fs for $\mathbf{1}H_2$ and 9 ± 3 ps for $\mathbf{1}H_4^{2+}$. The significant red shift of the Soret ($\Delta\lambda \sim 15$ nm) and *Q* absorption bands of $\mathbf{1}H_2$ compared to the parent $TPPH_2$ was also interpreted as a clear evidence of the strong electronic coupling between the porphyrin π system and the ferrocenyl moieties. According to several authors, the downfield shift of the ^{1}H NMR signal corresponding to the internal NH as well as the merging and bathochromic shift of the *Q* bands in the electronic absorption spectrum of $\mathbf{1}H_2$ reflect the electronically and sterically induced decrease of the porphyrin-based ring current effect [17,18,23]. The X-ray structure of the α,β,α,β-free base porphyrin $\mathbf{1}H_2$ [18] revealed especially the tilted conformation of the ferrocene groups characterized by a dihedral angle of around 35° and the saddle shape of the porphyrin macrocycle in the solid state. A variable temperature ^{1}H NMR study of $\mathbf{1}H_2$ [23] further revealed that the absence of alkyl groups at the β-positions of the porphyrin skeleton allows a free rotation of the ferrocene subunits around the C(*meso*)–C(Fc) bond at room temperature. Upon decreasing the temperature, the β-pyrrolic proton signal underwent two successive decoalescence processes corresponding to the progressive slowing of the ferrocene rotation (223–213 K, $\Delta G^{\neq} \sim 10.4$ kcal mol^{-1}) and the well-known "freezing" of individual NH tautomers (<183 K, $\Delta G^{\neq} \sim 7.9$ kcal mol^{-1}). This redox active species showed expectedly a rich electrochemical signature which prompted diverse interpretations, but the accurate attribution of the electron transfer processes was significantly hampered by adsorption phenomena especially observed in dichloromethane [18]. Besides the positive potential shifts, due to purely electronic effects, of both ferrocene- and porphyrin-based redox couples in $\mathbf{1}H_2$ relatively to the reference ferrocene and $TPPH_2$, one of the most important conclusions of these studies is undoubtedly that the ferrocene groups are "communicating" through the conjugated porphyrin backbone, as proved by the observation of multiple redox waves corresponding to the successive oxidations of interacting ferrocenes. Such aspect was especially developed by Nemykin et al. who studied and characterized mixed valence species using Mössbauer spectroscopy, MCD and spectroelectrochemical methods [23,24].

The related zinc and copper complexes, readily formed with the free base $\mathbf{1}H_2$, have also been reported [23,25] and the

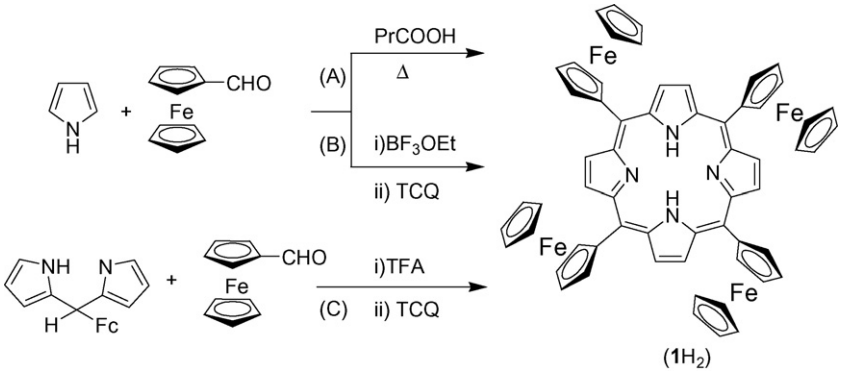

Fig. 1. Synthesis of $\mathbf{1}H_2$ from ferrocene carboxaldehyde according to three different strategies: (A) [15], (B) [12] and (C) [17,18].

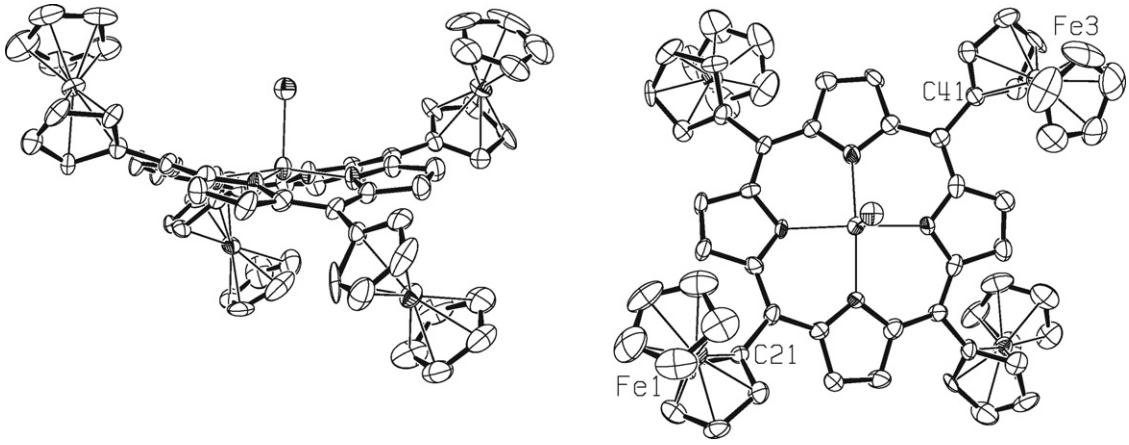

Fig. 2. Top and side ORTEP views of the [**1**Zn·THF] solid-state structure [26]. For clarity reasons, hydrogen along with THF carbon atoms were omitted. Thermal ellipsoids are scaled to the 40% level probability.

solid-state structure of [**1**Zn·THF] was recently determined in our group [26] (Fig. 2). As previously observed for the free base, the molecule adopts an α,β,α,β conformation and the porphyrin shows a saddle deformation with a distance between the zinc(II) atom and the N4 mean plane of 0.27 Å. The torsion angle Fe(1)–C(21)–C(41)–Fe(3) of the ferrocene subunits located on the THF ligand side is 57.4° and the distance between the α,α and β,β ferrocene iron atoms are respectively 11.73 and 11.52 Å.

The interest towards molecules showing multiple interacting redox centres prompted the development of strategies enabling the synthesis of various partially *meso*-substituted ferrocene porphyrins [27]. A mixture of mono-, bis- and tris-ferrocenyl-substituted porphyrins could especially be obtained from the reaction of 5-ferrocenyldipyrromethane with benzaldehyde (**2**H_2, **3**H_2, **4**H_2, **5**H_2, Fig. 3) [28]. The poor solubility of the mixture components precluded their efficient separation by chromatography and only **2**H_2 and **5**H_2 could be obtained as pure samples. Using similar synthetic strategies, the introduction of 4-methyl-, mesityl- or 4-*tert*-butyl-benzyl-groups at the *meso* positions proved later to allow cleaner and easier separations of all these components [17,26,27,29].

The 5,10-diferrocenyl-15,20-diphenylporphyrin (**3**H_2, Fig. 3) was recently isolated and its electrochemical or chemical one-electron oxidation was shown to produce a red shift of the Soret band, from 426 to 452 nm, and the disappearance of the *Q* bands, along with the appearance of new bands at 803 nm attributed to an IVCT band of a mixed valence Fe(II)–Fe(III) species [24]. The effect of intimate connection between porphyrin and ferrocene is also well illustrated by the relative positive potential shift $\Delta E \sim 100$ mV of the $P/P^{\bullet+}$ redox couple measured between TPPZn and the monoferrocenyl species **2**Zn and by the similar negative potential shift measured for the $P/P^{\bullet-}$ couple between TTPZn and **1**Zn. The metallocene group thus clearly makes the aromatic azamacrocycle harder to oxidize and to reduce. This increase of the porphyrin-based HOMO–LUMO gap can be easily understood upon considering the electron donating properties of ferrocene and the opposite withdrawing effect of electrogenerated ferrocenium group. Similarly the electron withdrawing porphyrin shifts the oxidation of ferrocene subunits towards positive potentials [26]. The porphyrin and ferrocene centred redox processes are furthermore sensitive to the porphyrin substitution pattern. The introduction of electron withdrawing pentafluorophenyl fragments at the porphyrin *meso* positions [30–32], following a Lindsey-like procedure similar to that described in Fig. 1(B and C) renders the porphyrin ring easier to reduce and the ferrocene groups harder to oxidize as would be expected. It especially showed that the resolution of the successive ferrocene-based oxidation waves could be modulated by the electrolyte. Using a dichloromethane solution of $[N(n\text{-}Bu_4)][B(C_6F_5)_4]$ as electrolyte, the potential difference measured between the successive ferrocene oxidations in **11**H_2 or **12**H_2 was *ca.* 0.1 V whereas these two metallocene centered process could not be resolved in a more polar acetonitrile $[N(n\text{-}Bu_4)][PF_6]$ electrolyte.

Ferrocene groups have also been successfully linked to the *meso* positions of β-alkylated porphyrins. The first example of β-alkylated ferrocene–porphyrin conjugate successfully synthesized was described by Boyd et al. [33]. The 5,15-di(ferrocenyl)-2,8,12,18-tetrabutyl-3,7,13,17-tetramethylporphyrin **18**H_2 (Fig. 4), formed according to a classical condensation between ferrocenecarboxaldehyde and a tetraalkyl dipyrromethane, was isolated and characterized in the solid state as a single isomer with both ferrocenyl fragments in a *syn* configuration with respect to the porphyrin ring (α,α-atropoisomer). The α,β-atropoisomer was not observed and according to the authors, the methyl groups at β pyrrolic positions offer sufficient steric hindrance to prevent any isomerisation process. The ferrocenyl and methyl substituents, respectively at the porphyrin *meso* and β positions, not only prevent the rotation of the metallocenyl but also lead to a strongly ruffled porphyrin core. The electrochemical study of **18**H_2 revealed two successive, ferrocene-centred, one-electron transfers separated by 0.19 V. This behaviour suggests the existence of unusually strong electronic interactions between both ferrocenyl substituents, the oxidation of the first metallocene making the second one harder to oxidize. This redox splitting turned out to be even more pronounced in the corresponding Ni(II) complex, **18**Ni, wherein the half wave potentials splitting reached 0.41 V. A spectroelectrochemical UV–vis investigation conducted on **18**H_2 and **18**Ni provided evidence for the

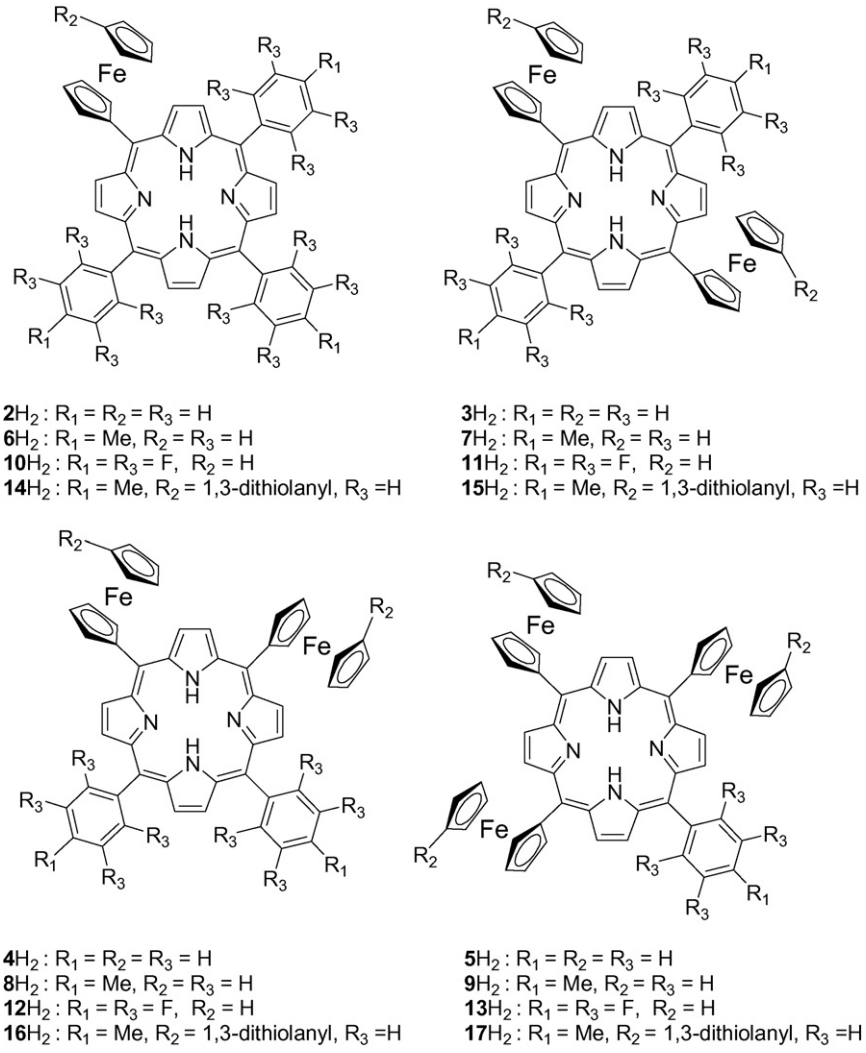

Fig. 3. Mixed ferrocene-containing porphyrins.

electrochemically driven formation of a mixed valence species characterized by absorption bands in the near infrared region (between 950 and 1100 nm). Studies on related systems (**19**H_2 and **20**H_2, Fig. 4) [34–36] have further shown that the potential difference between the ferrocene-based redox couples can be tuned by the nature of the inserted metal cation.

This exceptional communication between two ferrocene groups facing each other has been explained in part by the rotational hindrance of the ferrocene caused by the alkyl groups in the β-position of the macrocycle and by an extensive mixing of both ferrocenyl molecular orbitals with that of the porphyrinic π-connector. The direct linkage between ferrocenyl and porphyrin fragments and the electron donating features of the alkyl groups is also responsible for a negative shift of the ferrocene redox potential as compared to the reference unsubstituted ferrocene. Although the activation barrier corresponding to the

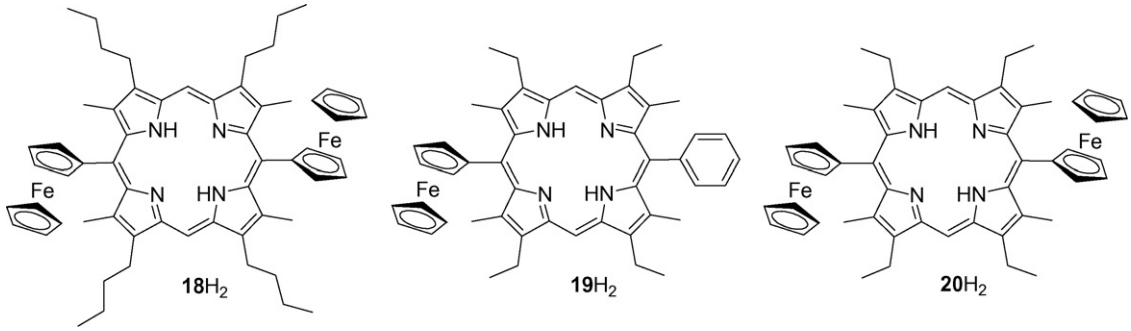

Fig. 4. Examples of β-alkylated porphyrin–ferrocene conjugates **18**H_2 [33], **19**H_2 [35] and **20**H_2 [34].

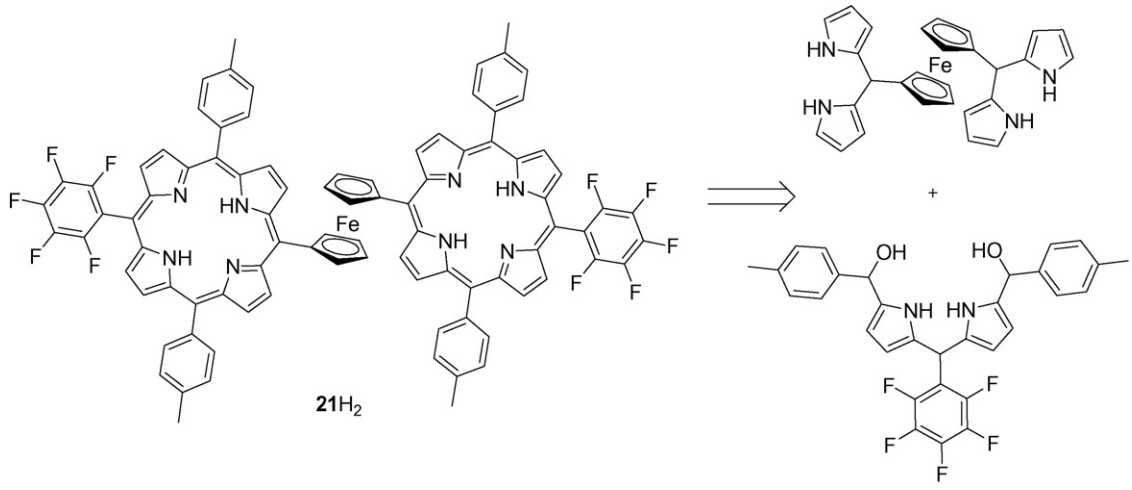

Fig. 5. Retro synthetic scheme corresponding to the preparation of the ferrocene bridged bis-porphyrin **21**H_2 [38].

rotation of ferrocene in such β-alkylated conjugates has never been evaluated, variable temperature ^{1}H NMR experiments conducted on **19**H_2 allowed the assessment of the activation energy (12.2 kcal mol^{-1}) corresponding to the porphyrin-based NH tautomerism process which matches that found for *meso*-tetraphenylporphyrin (TPPH_2) or octaethylporphyrin (OEPH_2) [37].

Owing to its unique dynamic and structural properties, the incorporation of a ferrocene group as bridging unit in face-to-face porphyrins has been a challenging objective for quite a long time. The synthesis of **21**H_2 has recently been reported in 18% yield by Koszarna et al. starting from a 1,1′-bisdipyrromethane synthon (Fig. 5) [38]. Based on variable temperature ^{1}H NMR experiments, the authors assume the absence of rotation around the ferrocene–porphyrin linkage.

The cyclic voltammogram of this ferrocene-bridged bis-porphyrin **21**H_2, recorded at high scan rates, is characterized by three irreversible anodic waves centered successively on the ferrocene moiety and on the porphyrin rings. Surprisingly, the reversibility of the ferrocene centred process turned out to be improved at lower scan rates as a possible consequence of a conformational re-arrangement which occurs at the time scale of the low scan rates. Following a similar strategy, the same authors reported an original pacman-type ferrocene bridged porphyrin–corrole in which the metallocene fragment is directly linked to both macrocycles [39]. NMR and UV–vis investigations on the latter revealed an improved conformational freedom compared to the bis-porphyrin analogue **21**H_2, and a poor electronic interaction between the ferrocene and corrole fragments.

Recently, supramolecular architectures comprising three porphyrin units bridged by two directly linked ferrocene have been synthesized [40] from a ferrocenecarboxaldehyde-subtituted porphyrin **22**H_2 and a dipyrromethane synthon (**23**H_6 and **24**H_6, Fig. 6). Metallation of **23**H_6 with Zn^{2+} led to the spontaneous and exclusive formation of the dimeric (**23**Zn_3)$_2$ species by complementary coordination. Addition of pyridine prompted a cleavage of the latter which could be converted into a series of macrocycles from dimer to decamer. The structures of supramolecular rings obtained from **24**H_6 could be further confirmed by mass spectrometry and STM analysis of reinforced systems produced by covalent linkage [41]. A systematic series of ferrocene functionalized Zn-imidazolyl porphyrins were further designed to self-assemble into slipped cofacial dimers through a similar supramolecular approach [42]. The authors additionally demonstrated the relevance of ferrocene-appended porphyrin cofacial dimers grafted onto ITO electrodes as cascade architecture to generate anodic photocurrent [43].

Upon studying different spacers between the macrocycle and the metallocene [42,43], Kalita et al. showed that a direct linkage induces the most important changes in the electrochemical and spectroscopic signatures of both moieties, making notably oxidation and reduction of the porphyrin ring harder, and causing a significant blue shift of all the absorption bands and a full fluorescence extinction. In the course of this work, the authors reported the first example of a porphyrin directly connected to a per-alkylated ferrocene fragment exhibiting consequently an exceptional red shift of the porphyrins *Q* bands as well as an important cathodic shift of the ferrocene oxidation wave.

The relevance of directly connected ferrocene–porphyrin conjugates in the field of molecular electrochemical sensing has been further demonstrated upon considering "redox picket-fence" porphyrins as multipoint recognition architectures. Such molecular systems combining several complementary binding sites and redox active reporters are indeed of the greatest interest to improve both recognition and detection ability of chemosensors. A multipoint molecular recognition event could potentially be followed and signaled by different redox-active probes distributed at strategic location on the receptor. The electrochemical, spectroscopic, and chemical features of ferrocene–porphyrin conjugates make them outstanding candidates to reach such goals. Besides the great chemical stability, the well-defined redox characteristics and chemical versatility of both ferrocene and porphyrin fragments, the generation of cationic species upon electrochemical oxidation of both moieties are moreover especially favourable to the strengthening of anion–receptor interactions [5].

The redox picket-fence porphyrin **25**H_2 was synthesized in four steps starting with the mono-protection of diformyl fer-

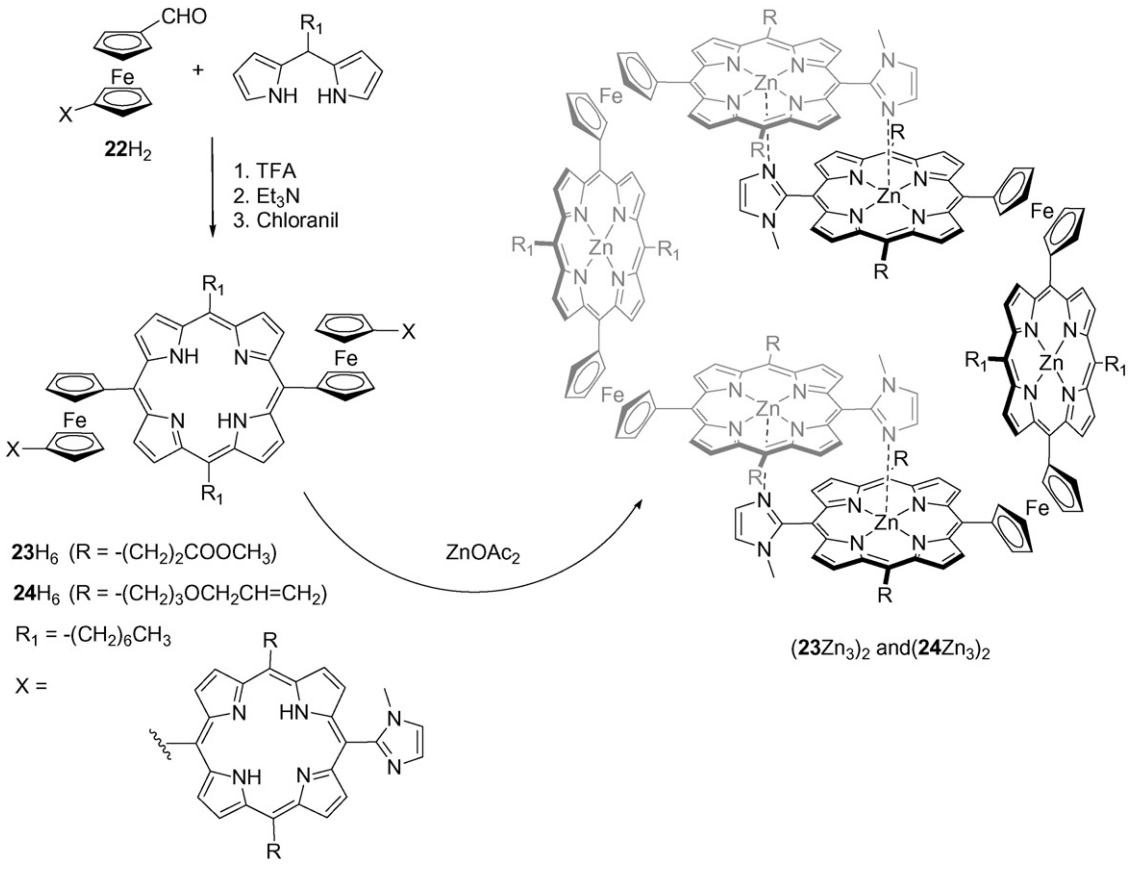

Fig. 6. Synthesis of tris-ferrocenyl porphyrins **23**H_2, **24**H_2 and the related metallated species [40].

rocene [44]. Condensation of the latter with tolyldipyrromethane in the presence of TFA, followed by oxidation with chloranil, afforded the scrambled ferrocene-substituted porphyrin derivatives **14**H_2, **15**H_2, **16**H_2 and **17**H_2 (Fig. 3) from which **14**H_2 was isolated with an 8% yield. **25**H_2 was then obtained from **14**H_2 by removal of the cyclic dithioketal and a nitrogenous "tail" was introduced onto the ferrocene moiety by reaction of *n*-hexylamine with the regenerated formyl group to produce an intermediate which was immediately reduced with an excess of $NaBH_4$ giving **26**H_2 (Fig. 7).

The self-assembling properties of the metallated derivative **26**Zn, coupled to an efficient electronic communication throughout the receptor, allowed an unprecedented ferrocene-based electrochemical sensing of neutral species *via* a metalloporphyrin-centred "tail on–tail off" binding process [45]. The secondary amine function in **26**Zn could be further quaternized to afford **27**Zn, an ammonium–ferrocene–metalloporphyrin chemosensor [46] specially suited to achieve an efficient electrochemical sensing of anionic species through a sensitive assessment of the anion electrostatic and nucleophilic features (Fig. 7). The well defined electrochemical signature of this assembly associated to a strong reinforcement of the anion binding properties upon oxidation, that produces up to three additional positive charges delocalized throughout the receptor, have thus been proved to be useful for the electrochemical recognition of specific anions and confirmed the efficiency of the multipoint anchorage strategy based on ion pairing effects and metal-ligand binding.

2.2. Linkage through conjugated spacers

The first strategy to introduce a conjugated spacer between ferrocene groups and a porphyrin involved 4-ferrocenylbenzaldehyde as building block (Fig. 8) [47]. The objective 5,10,15,20-tetrakis(4-ferrocenylphenyl)porphyrin **28**H_2 was synthesized in 15% yield using a classical Adler and Longo [16] method upon refluxing pyrrole and 4-ferrocenylbenzaldehyde in propionic acid. Upon introducing an appropriate mixture of aldehydes, the same stategy allowed D'Souza et al., more recently, to isolate the related 5,10,15-triphenyl-20-(4-ferrocenylphenyl)porphyrin in *ca.* 6% yield [48].

As a result of the absence of communication between the ferrocenes and the porphyrin ring, all four chemically equivalent ferrocenes are electrochemically oxidized at the same apparent potential and the UV–vis spectrum of this compound was found to be similar to that of the simple 5,10,15,20-tetraphenylporphyrin. Different authors used the same ferrocene containing building block or analogues in Lindsey-like mixed condensation of one dipyrromethane and two different aldehyde groups to synthesize ferrocene containing AB_2C porphyrins with potential applications as molecular multibit information storage units [29,42,49]. Related molecules

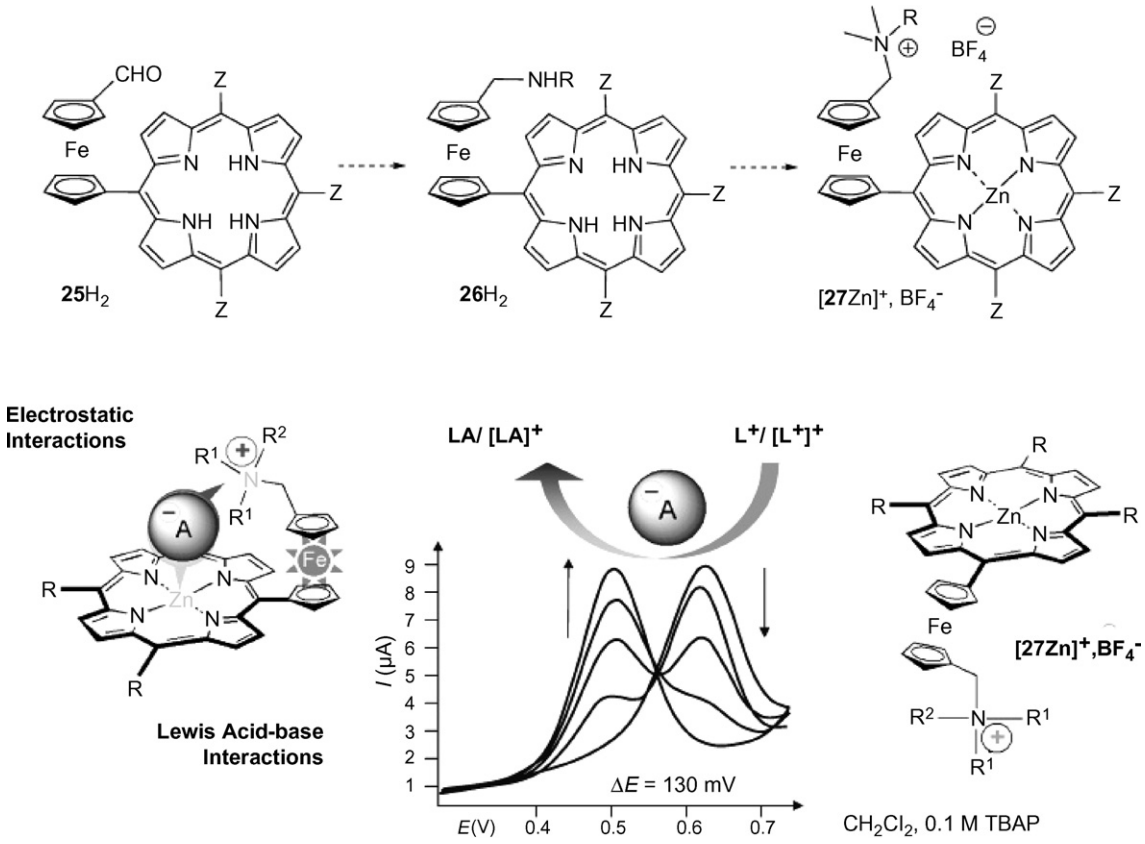

Fig. 7. Synthesis and schematic electrochemical recognition properties of the redox picket-fence porphyrin [**27**Zn]$^+$ [45,46].

like the thiol (for surface attachment) derivatized bisferrocenyl porphyrin **29**H_2 could alternatively be obtained starting from a 5(4-ferrocenyphenyl)dipyrromethane and various aldehydes [29,48]. The *in situ* deprotection of the *S*-acetyl group or *S*-(*N*-ethylcarbamoyl) protecting groups on gold surfaces afforded robust self-assembled monolayers (SAM) characterized by three reversible, ferrocene- and porphyrin-centred electron transfers. A porphyrin bearing mono benzylphosphonic acid tether and phenyl-ferrocene subunits were similarly prepared for attachment to metal oxide surface, but the poor solubility of the targeted zinc complex greatly limited its characterization and use [50]. The introduction of phenyl linkers did not allow information exchange between the ferrocene and the macrocycle and the electrochemical properties of these molecular assemblies grafted on gold electrode or SiO_2 surfaces consequently do not differ from those of the separated elements.

Another effective strategy to introduce ferrocene fragments at the periphery of a porphyrin through conjugated linkers takes advantage of palladium-based Sonogashira coupling reactions. A triad containing a zinc porphyrin input unit, a phthalocyanine output and ferrocene as redox switching unit could be obtained in 15% yield through such palladium mediated coupling between

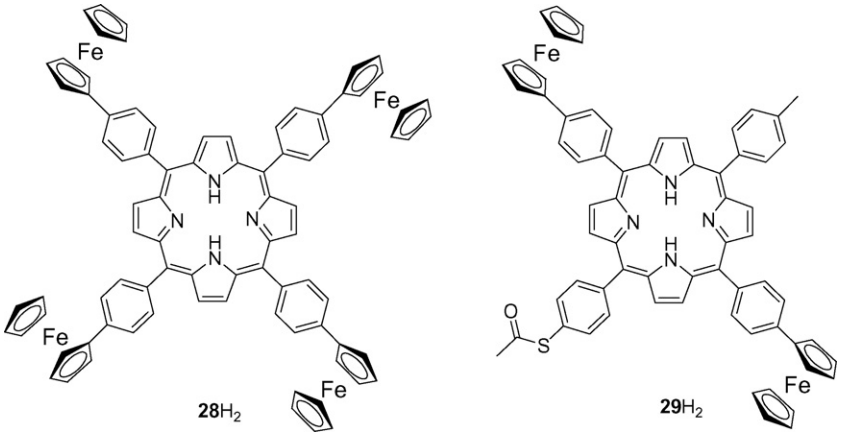

Fig. 8. Ferrocenylphenyl containing porphyrins **28**H_2 [47] and **29**H_2 [29].

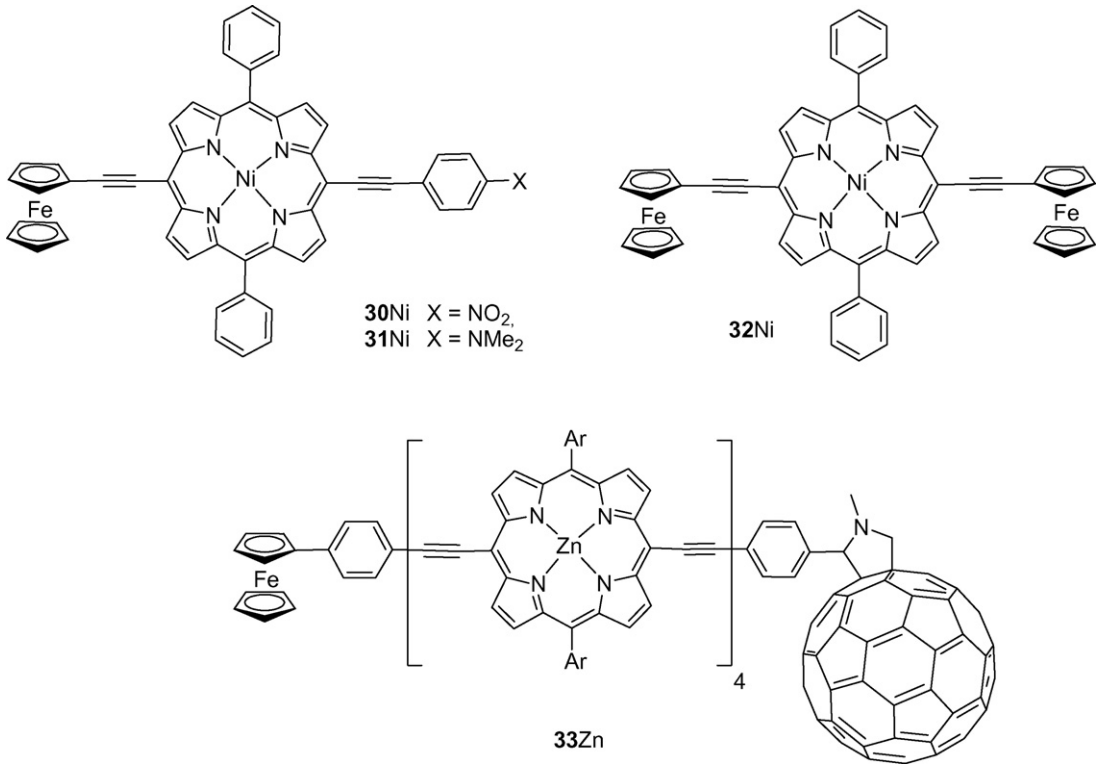

Fig. 9. Ethynyl bridged ferrocene–porphyrin derivatives obtained using a Sonogashira coupling methodology [52].

ethynyl substituted ferrocene and phthalocyanine and a 5,20-bis(4-iodophenyl)porphyrin derivative. This compound was developed by Ambroise et al. [51] as a porphyrin-based optoelectronic gate which could be studied without causing quenching of the excited state energy migration along the energy transfer train in the porphyrin-based molecular wire of the device. A similar approach was further developed to synthesize the potentially "push–pull" NLO chromophores **30**Ni and **31**Ni [52], as well as the bis ferrocenyl analogue **32**Ni obtained in 66% yield starting from a (5,15-dibromo-10,20-diphenylporphyrinato)nickel(II) and ferrocenylethyne [53] (Fig. 9). Conjugated porphyrin-based molecular wires in which a ferrocene, as electron donor, and a fullerene, as electron acceptor, connected *via* butadiyne-linked porphyrin oligomers were likewise recently synthesized from silicon-terminated oligomers using a Sonogashira coupling methodology (**33**Zn, Fig. 9) [54].

The X-ray crystal structure of **30**Ni revealed a large dihedral angle of 85.7° between the lower rim ferrocene-based cyclopentadiene and the porphyrin plane. This nearly orthogonal arrangement observed at the solid state led the authors to conclude that ferrocene may not function as a good electron donor in such a system [52]. The lack of redox interaction between the metallocene groups in the bis ferrocenyl **32**Ni, revealed by a single oxidation wave corresponding to the oxidation of both iron centres, was interpreted as the result of the large Fe–Fe distance estimated around 19 Å [53].

Giasson et al. [55] used a Wittig condensation between a ferrocene ylide and an aldehyde containing porphyrin to associate both fragment through a conjugated linker (**34**H_2, Fig. 10). Starting from **34**H_2 and its reduced analogue **35**H_2, they investigated the nature and efficiency of the porphyrin excited state quenching by ferrocene. Steady state emission spectroscopy and Stern–Volmer analysis especially revealed that the quenching of the ethyl linked derivative **35**H_2 is half as fast as the vinyl trans-linked analogue **34**H_2. The authors also concluded from this investigation that the ferrocene centre in both derivatives quenches the singlet excited state of the porphyrin through an electron transfer mechanism.

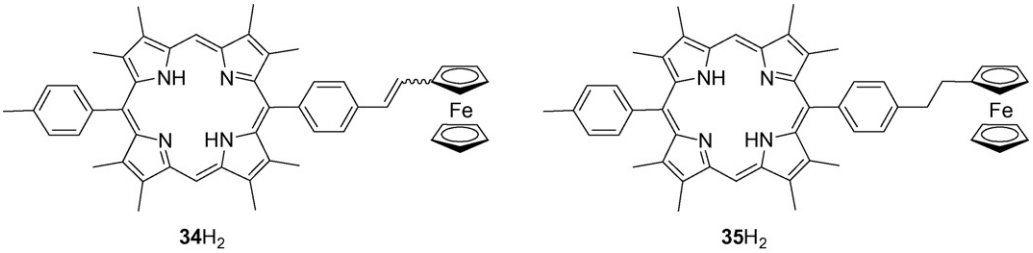

Fig. 10. 5-Ferrocenylvinylphenyl-15-tolyl-2,3,7,8,12,13,17,18-octamethylporphyrin **34**H_2; 5-ferrocenylethyl-phenyl-15-tolyl-2,3,7.

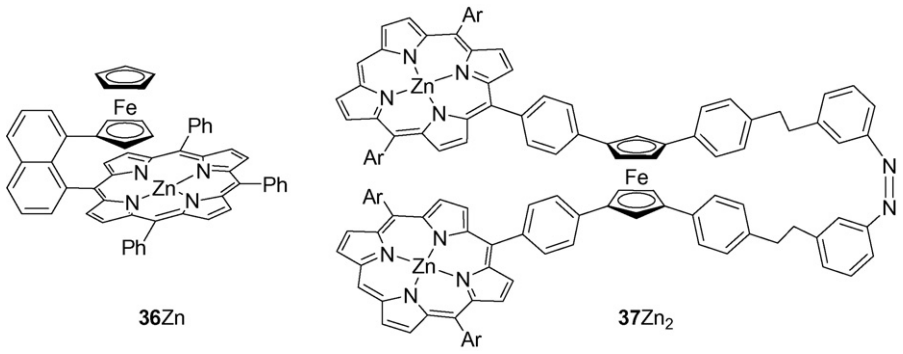

Fig. 11. Model for heterobimetallic polymers **36**Zn [57] and Muraoka's light powered molecular pedal **37**Zn_2 [58].

Both structures have also been successfully associated through a conjugated Schiff base linkage by condensing mono (*ortho*- and *para*-aminophenyl)porphyrins and ferrocene carboxaldehyde to produce different "picket-fence" isomers of a mono ferrocenyl Schiff base porphyrin [56].

A naphthalene linker has recently been introduced in a porphyrin–ferrocene dyad in order to achieve, for the first time, a face-to-face contact between both redox active systems providing a model for heterobimetallic polymers based on the same repeating unit. The targeted conjugate **36**Zn (Fig. 11) could be obtained in 18% yield through a Suzuki coupling between a *meso*-5-[8-triflate-naphthalenyl]-10,15,20-triphenylporphyrin and ferrocene bis(boronic acid) [57]. The location of the ferrocene in the porphyrin-based anisotropic cone could be easily confirmed by ^{1}H NMR through the strong shielding of the cyclopentadienyl protons observed between 0 and 3.3 ppm.

Muraoka et al. [58] reported an interesting use of the ferrocene mechanical properties in designing and synthesizing the light powered molecular pedal **37**Zn_2 (Fig. 12) whose conformational changes and mechanical twisting could be induced by photoisomerization of the azobenzene group. The key step of this synthesis is a palladium catalyzed coupling reaction between a dibromoferrocene derivative with a zinc porphyrin boronate to produce the ferrocene bridged bis-porphyrin **37**Zn_2 (Fig. 12).

2.3. Linkage through saturated spacers

One of the first examples of ferrocene–porphyrin assemblies linked by a non-conjugated spacer is the bis-porphyrin **38**H_2 (Fig. 12) reported by Beer and Kurek [59]. This "face-to-face" porphyrin bridged by a ferrocenyl group was obtained by condensation of 1,1′-bis(chlorocarbonyl)ferrocene with two equivalents of 5-(*p*-hydroxyphenyl)-10,15,20-triphenylporphyrin [59]. Based on the same strategy and starting materials, the authors [60] also described the synthesis and characterization of the porphyrin–ferrocene–quinone **39**H_2 associating multiple electron donors and acceptors via ester linkages (Fig. 12).

This concept was further developed by Wagner et al. [61,62] who used a ferrocene containing fragments as a redox active strap joining two adjacent *meso* positions of a porphyrin skeleton. The acid catalysed condensation of pyrrole with ferrocene and quinone linked bisbenzaldehyde especially afforded strapped porphyrins like **40**H_2, **41**H_2 and **42**H_2 (Fig. 13). The expected atropoisomers of bisferrocene strapped porphyrins like **41**H_2 could not be isolated from the racemic mixture.

Numerous porphyrin-based architectures displaying donor and acceptor groups have then been developed as synthetic models of the natural photosynthetic system [63,64]. Investigations of photoinduced electron transfer in ferrocene–porphyrin–fullerene linked molecules have especially attracted enormous interest to address mechanistic issues,

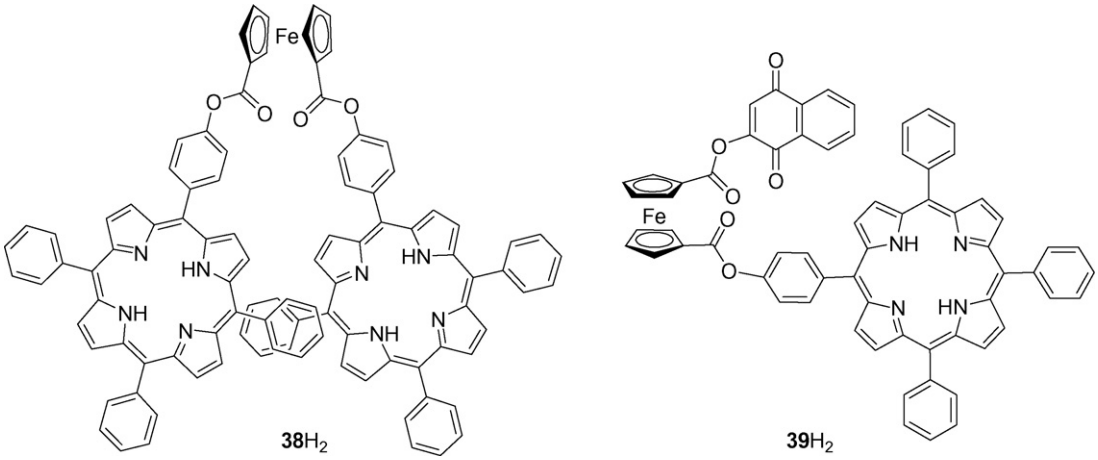

Fig. 12. Ferrocene–porphyrin assemblies linked by non-conjugated spacers [59,60].

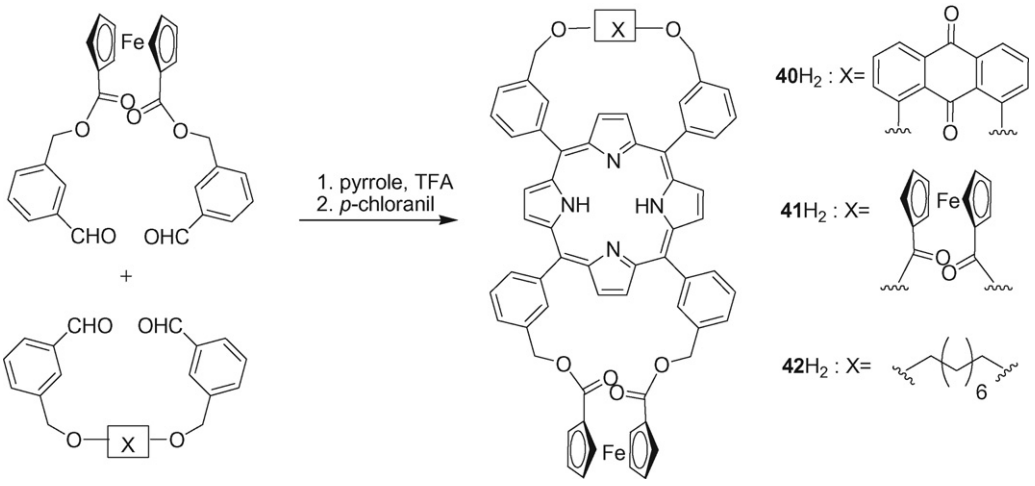

Fig. 13. Ferrocene-strapped porphyrins [61,62].

or to develop artificial solar energy conversion processes. Most of these molecular architectures were synthesized by reacting ferrocene aniline derivatives with appropriate porphyrin-based starting materials (monomer, dimer, trimer, etc.) bearing at least one acid chloride group in *meso* position [48,65–74]. An inverse approach, which leads to similar molecular structures, involves the use of chlorocarbonyl-; 1,1′-bischlorocarbonyl- or [4-(chlorocarbonyl)phenyl]-ferrocene with *meso*(4-aminophenyl)- or *meso*(4-hydroxyphenyl)porphyrins [75–79]. A representative ferrocene–porphyrin–fullerene sequence synthesized by Imahori et al. [73] to achieve long distance charge separated states is shown in Fig. 14. These strategies based on amide bond formation are the most widely used, but one find a few examples of covalently linked ferrocene porphyrins obtained from halogenated ferrocene derivatives and phenol containing porphyrins [80–83] or using more classical Lindsey-like porphyrin syntheses with the appropriate ferrocene-linked aldehydes [42]. Ferrocene-appended pyridine fragments have also been covalently connected to a supramolecular metalloporphyrin tetramer in two steps, starting with a non-covalent metalloporphyrin–pyridine-based interaction followed by an olefin metathesis between the porphyrin and ferrocene containing subunits [84].

For the first time, the authors reported a light harvesting porphyrin trimer incorporated into a photosynthetic electron transfer model including ferrocene as electron donor, and a fullerene as an electron acceptor. Light irradiation of this ferrocene-*meso*,*meso*-linked porphyrin trimer–fullerene pentad **43**Zn_3 resulted in an intramolecular photoinduced electron transfer from the singlet and triplet excited states of the central trimer to the fullerene fragment, affording the separated charge species $Fc–(ZnP)_3^{\bullet+}–C_{60}^{\bullet-}$. The electron transfer from the ferrocene centre to the $(ZnP)_3^{\bullet+}$ fragment led then to the separated charge species $Fc^{+}–(ZnP)_3–C_{60}^{\bullet-}$. This process competes with the back electron transfer between the $C_{60}^{\bullet-}$ and $(ZnP)_3^{\bullet+}$ fragments but the quantum yield corresponding to the formation of the final $Fc^{+}–(ZnP)_3–C_{60}^{\bullet-}$ species was estimated at 83% in benzonitrile with a exceptionally long life time of 0.53 s at 163 K in DMF.

Another very interesting application of covalently connected ferrocene–porphyrin architectures deals with the electrochemical recognition of specific targeted species. Beer et al. [11] reported the first example of such redox-active receptor (**44**Zn, Fig. 15) based on of ferrocenyl-substituted atropoisomers of 5,10,15,20-tetrakis(2-aminophenyl)porphyrin Zn(II) (TAPP).

Through measurable modifications in the electroactivity of the ferrocene subunits, linked to the porphyrin skeleton by amide spacers, the electrochemical detection and titration of anionic species in acetonitrile media were achieved through a combination of different complementary interactions, namely

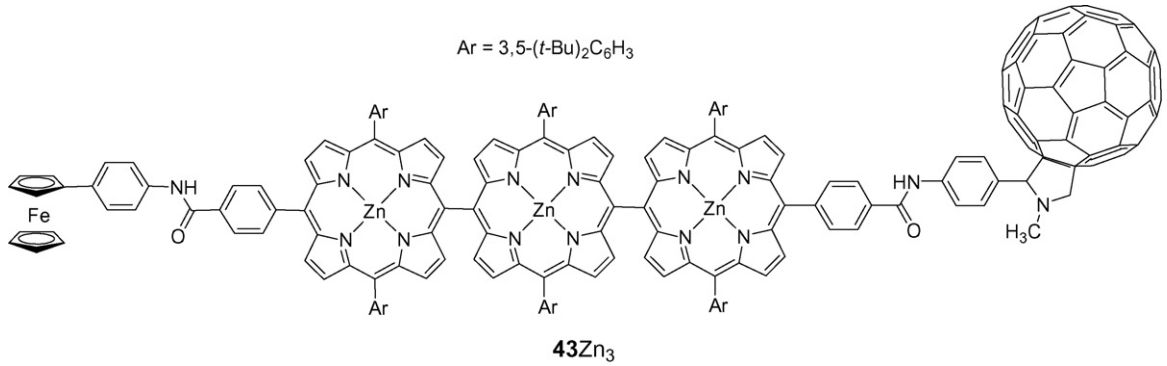

43Zn_3

Fig. 14. Ferrocene–porphyrin trimer–fullerene pentad **43**Zn_3 developed by Imahori et al. [73].

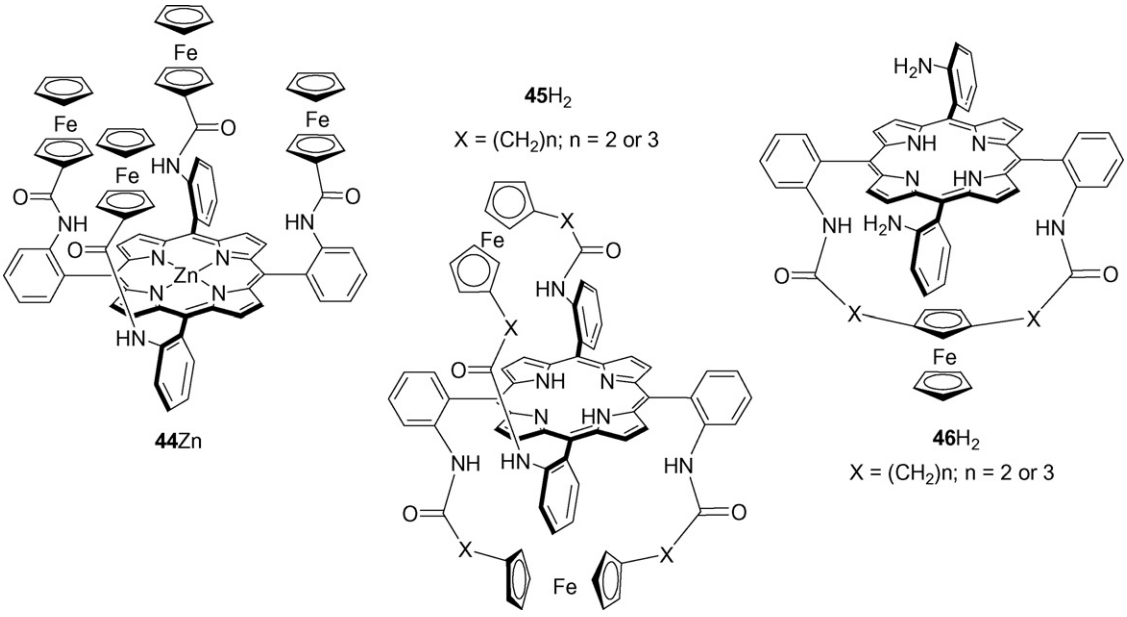

Fig. 15. Ferrocene containing picket-fence porphyrins **44**Zn [11,85], **45**H_2 and **46**H_2 [86].

coordination to the metal centre and hydrogen bonds between anions and amide subunits. Interestingly, the selectivity and efficiency of the anion recognition process was dependent on the form of the atropoisomeric receptor [85].

The use of $TAPPH_2$ atropoisomers as starting material for the elaboration of ferrocene–porphyrin conjugates was first developed by Hisatome et al. who successfully synthesized ferrocene-bridged porphyrins as **45**H_2 or **46**H_2 wherein two opposite amino groups were connected to both cyclopentadiene (Cp) or to the same Cp of a metallocene fragment [86].

In the same vein, Hodgson et al. [87] reported a series of metal free and metallated ferrocenamido- and pivalamidophenylporphyrins starting from the α,α,α,α-5,10,15,20-tetrakis (*o*-aminophenyl)porphyrin and the α,α- and α,β-atropoisomers of the bis(aminophenyl)-2,8,12,18-tetrapropyl-3,7,13,17-tetramethylporphyrin. The solid-state structure of 5,10,15,20-tetrakis-(ferrocenamidophenyl)porphyrins Fe(III) especially revealed a bromide anion coordinated to the metal centre and H-bonded to four "picket-fence" amide functions.

2.4. Miscellaneous

The interest towards ferrocene–porphyrins has especially promoted the development of non-covalent assembling strategies. These investigations are partly inspired by the desire to reproduce natural photosynthetic reactions occurring along supramolecular assemblies in protein environments. One of the most straightforward approach takes advantage of the known ability of metalloporphyrins to bind axial coordinating fragments.

The number and nature of suitable ligands are metal dependant and one find a variety of ferrocene containing moieties able to interact with TPP- or OEP-derived metalloporphyrins wherein M could be zinc(II) [88,89], iron(III) [90], or Gallium(III) [90]. Upon deprotonating the metallocene fragment, a direct cyclopentadiene–metal bond has also been observed with a germanium β-peralkylated porphyrin [91–94]. The reported mono-ferrocene and bis-ferrocene metalloporphyrins (**47**Ge, Fig. 16) wherein the metallocene groups are σ-bonded to the germanium atom showed unexpected photostabilities presumably driven by porphyrin to ferrocene energy transfers. Moreover, the electrochemical characterization of the metalloporphyrin bridged bis ferrocene **47**Ge revealed a strong communication between both iron centres ($\Delta E = 180$ mV) as well as an unusual cathodic shift of the first ferrocene oxidation potential.

The coordinating properties of peripheral functional groups attached to a porphyrin ring was also used to build self-assembled porphyrin–ferrocene architectures. Supramolecular complexes were especially obtained through metal mediated self-assembly of pyridyl-*meso*-substituted porphyrins and 1,1′-bis(diphenylphosphino)ferrocene [95]. Schmittel et al. [96] recently designed phenanthroline-linked porphyrin scaffolds which were combined with bis-ferrocenyl module through Cu(I)-mediated heteroleptic bisphenanthroline complexation (**48**–**52**Zn, Fig. 16). The association between both redox active chromophores was likewise achieved through hydrogen bonding between a barbiturate functionalized porphyrin and the complementary polyamide ferrocene containing building block to produce **53**H_2 (Fig. 16) [97] wherein the distance between both chromophore was estimated to be ∼23 Å.

3. β-Pyrrole-linked ferrocene–porphyrins

Due to obvious synthetic impediments, the insertion of ferrocene fragments in β-pyrrolic positions of a porphyrin ring has been much less investigated. The first example of such association was reported by Burrell et al. [98,99] from a Wittig reaction between a TPP-derived phosphonium salt (**53**H_2) and formylferrocene or 1,1′-diformylferrocene, affording mono-

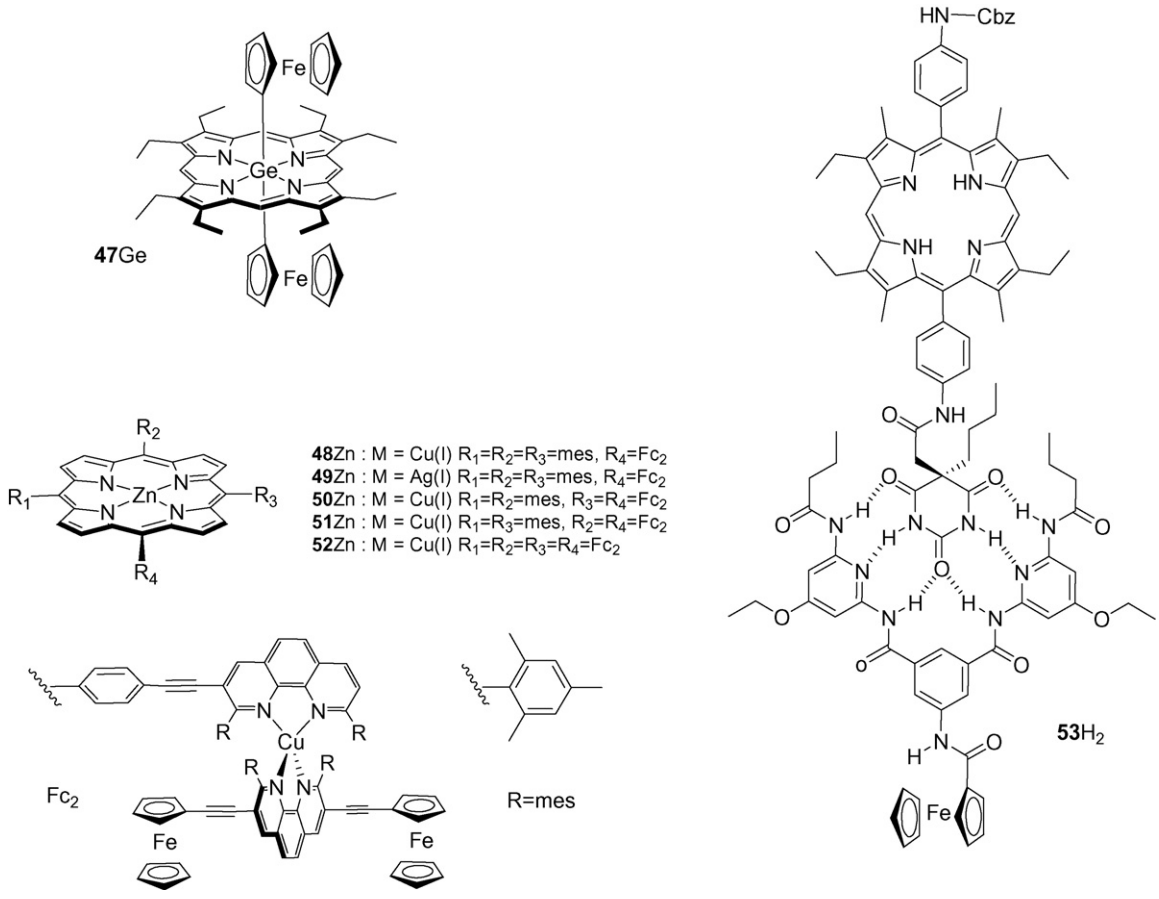

Fig. 16. Non-covalent ferrocene–porphyrin assemblies **47**Ge [91–94], **48**–**52**Zn [96] and **53**H_2 [97].

and bisporphyrin–ferrocene conjugates connected in β-pyrrolic position through ethylenic spacers (Fig. 17).

Smith and co-workers [13,14,100] recently reported a series of original conjugates in which the metallocene is fused to the porphyrin chromophore. Besides the synthetic challenge, such molecules were designed to enhance their interactions through a forced orbital overlap. The fused face-to-face ferrocene bridged bisporphyrin **57**Ni (Fig. 18) was especially obtained through

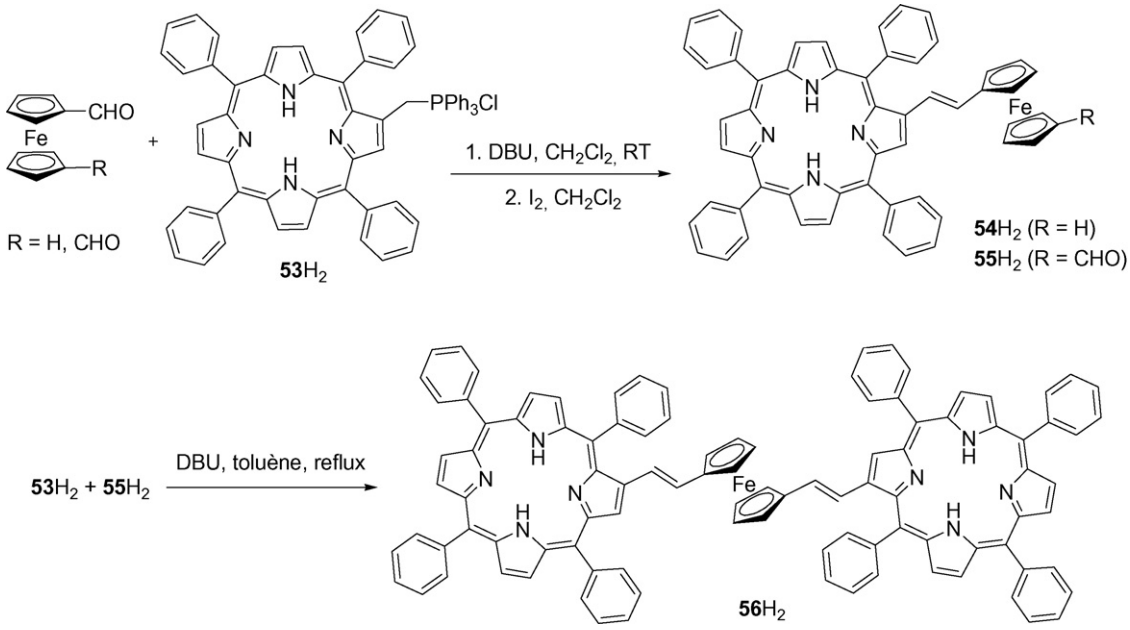

Fig. 17. Wittig-driven synthesis of 1,1′-bis(2-ethylenyl-5,10,15,20-tetraphenylporphyrin) ferrocene **56**H_2 [45].

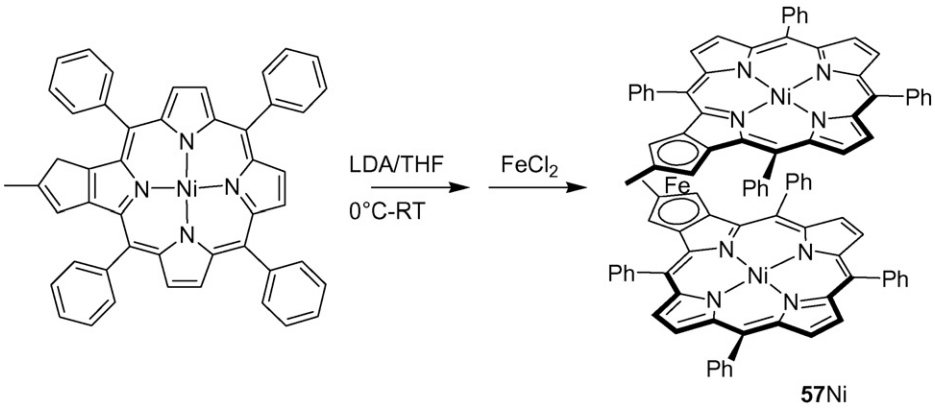

Fig. 18. Structure of a β,β′-"fused" bisporphyrin **57**Ni [13].

a palladium(0) catalyzed cycloaddition reaction generating a five-membered carbocycle in one step. Its deprotonation with LDA at low temperature and subsequent addition of $FeCl_2$ in the reaction medium afforded the desired porphyrin dimer in 30% yield. The electrochemical activity of the latter revealed strong interactions, not observed with the bis-copper or zinc analogues, between the π-rings of the two equivalent porphyrin macrocycles.

4. Ferrocene–porphyrin analogues

Although such an aspect lies beyond the scope of the present review, we choose to give a brief overview of molecular structures wherein ferrocene has been associated with porphyrin analogues. The potential applications of these new architectures are similar to those mentioned in the previous paragraphs and rely on the exciting binding, electronic, structural properties of original macrocycles with various sizes, conjugation and heteroatoms. This field is rapidly growing and numerous examples have been recently reported with analogues as oxasmaragdyrin [101,102], corroles [39], oxacorroles [101], porphodimethenes [34,117], tetraazaporphyrins and phthalocyanines [51,53,103–110] and others [111–113]. Some of these structures are depicted in Fig. 19.

With the aim of developing chemosensors, redox active hybrid macrocyclic architectures characterized by a direct connection between dipyrrin, tripyrrin and ferrocenyl fragments (Fig. 20) have recently been synthesized in our group [114]. Contrary to fully conjugated porphyrins, in which four pyrrole moieties contribute to the overall aromatic π-electronic

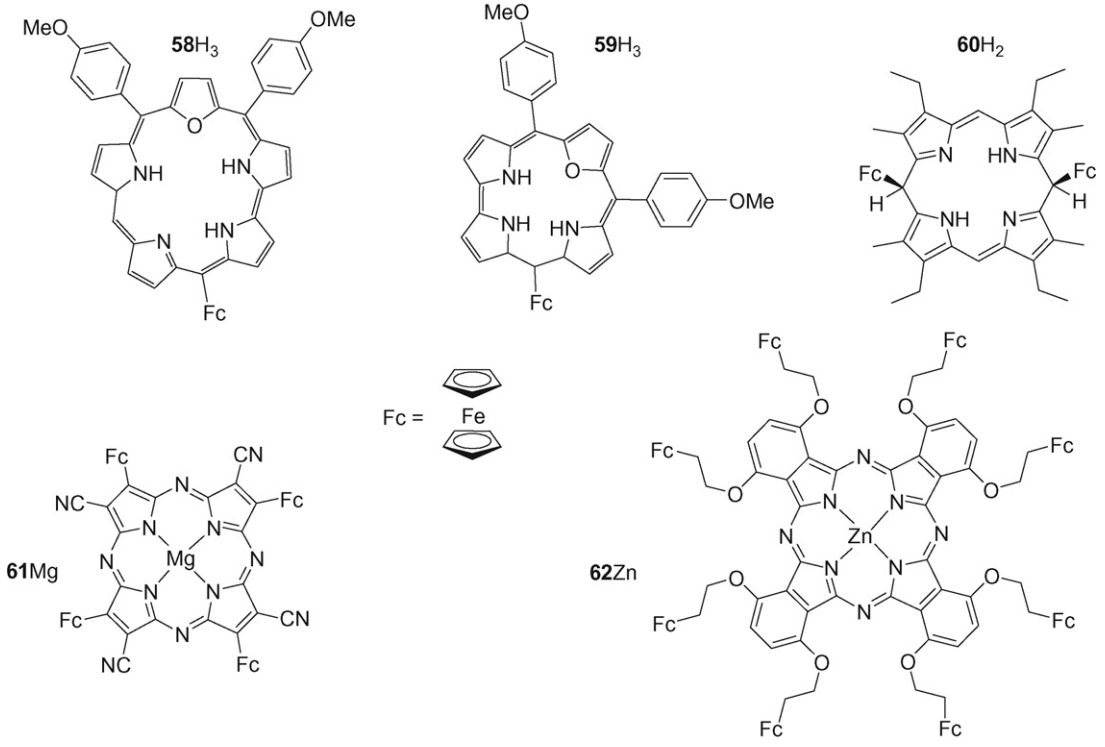

Fig. 19. Examples of association between ferrocene and porphyrin analogues [47,49,51,57].

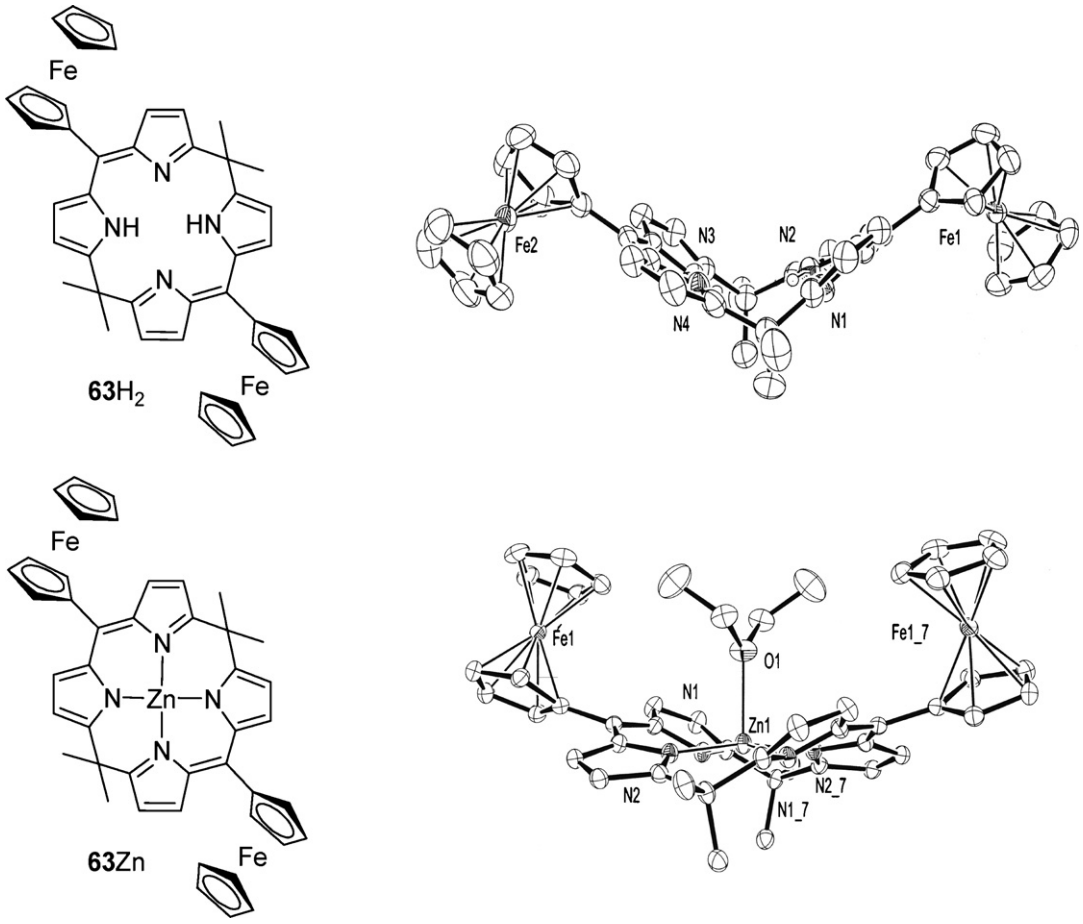

Fig. 20. Side Ortep views of the free base **63**H_2 and zinc complex **63**Zn of a *meso*-ferrocenylcalix[4]phyrines [114].

system and behave as a unique electroactive species, these calixphyrin [115] macrocycles, structurally related to calixpyrroles [116] and porphyrins, can be regarded as an assembly of independent redox active pyrrole and conjugated oligopyrrole fragments linked through sp^3 hybridized *meso* carbon atoms. The disruption of the conjugation pathway not only multiplies the number of redox centres throughout the molecule but also leads to a large variety of molecular architectures with specific physico-chemical properties. The corresponding ferrocene containing hybrid macrocycles exhibit especially attractive electronic and structural features suited for use as molecular sensing tools. An efficient voltammetric sensing of exogenic electron rich anionic species could especially be performed using a metallo-calix[4]phyrin through the displacement of the labile axial binding site, the perturbation of the $Fc^{0/+}$ redox couple being directly related to the complexed species features.

5. Conclusion

Molecular architectures based on the intimate association between totally or partially conjugated macrocycles and metallocenes fragments are highly interesting materials. Their unique electrochemical and UV–vis signatures as well as their switchable fluorescence properties have recently promoted the development of numerous assemblies. Ferrocene–porphyrin-based donor–acceptor linked structures have especially emerged as efficient artificial photosynthesis models owing to their ability to produce long-lived charge separated states and subsequent generation of photocurrent. Such association also holds great promise in the field of molecular sensing since the direct connection of an organometallic redox subunit to the π-electronic system of a conjugated macrocycle allows an optimised "communication' between both fragments. The extremely rich electrochemical activity of ferrocene-appended porphyrins can furthermore be considered as an increased memory density allowing multibit information storage. Ferrocene and porphyrins have been associated in a large number of architectures and their mutual influences and unique physico-chemical properties are well understood nowadays. Synthetic challenges have however recently been taken up with the syntheses of β-fused conjugates, ferrocene bridged bis-porphyrins or supramolecular architectures. Over the last years, increasing attention has also been devoted to devising synthetic pathways towards the parent ferrocene–porphyrin analogues and assessing their properties. These original structures not only open up exciting perspectives in the fields mentioned above, they will also undoubtedly provide fertile ground for the development of novel synthetic innovations and promising applications.

References

[1] M.R. Wasielewski, Chem. Rev. 92 (1992) 435.
[2] D. Gust, T.A. Moore, A.L. Moore, Acc. Chem. Res. 26 (1993) 198.
[3] J.R. Health, P.J. Kuekes, G.S. Snider, R.S. Williams, Science 280 (1998) 1716.
[4] Y. Chen, J. Jung, D. Ohlberg, X. Li, D.R. Stewart, K.A. Jeppesen, J.F. Stoddart, R.S. Williams, Nanotechnology 14 (2003) 462.
[5] P.D. Beer, P.A. Gale, G.Z. Chen, Coord. Chem. Rev. 185/186 (1999) 3.
[6] A.J. Bard, Nature 374 (1995) 13.
[7] K. Matsushige, H. Yamada, H. Tada, T. Horiuchi, X.Q. Chen, Ann. N. Y. Acad. Sci. 852 (1998) 290.
[8] Z. Liu, A.A. Yasseri, J.S. Lindsey, D.F. Bocian, Science 302 (2003) 1543.
[9] N.M. Loim, E.V. Grishko, N.I. Pyshnograeva, E.V. Vorontsov, M. Sokolov, Russ. Chem. Bull. 43 (1994) 871.
[10] N.M. Loim, M.A. Kondratenko, E.V. Grishko, M. Sokolov, Russ. Chem. Bull. 43 (1994) 905.
[11] P.D. Beer, M.G.B. Drew, D. Hesek, R. Jagessar, J. Chem. Soc., Chem. Commun. (1995) 1187.
[12] N.M. Loim, N.V. Abramova, V.I. Sokolov, Mendeleev Commun. (1996) 46.
[13] H.J.H. Wang, L. Jaquinod, D.J. Nurco, M.G.H. Vicente, K.M. Smith, Chem. Commun. 24 (2001) 2646.
[14] H.J.H. Wang, L. Jaquinod, M.M. Olmstead, M.G.H. Vicente, K.M. Kadish, Z. Ou, K.M. Smith, Inorg. Chem. 46 (2007) 2898.
[15] R.G. Wollmann, D.N. Hendrickson, Inorg. Chem. 16 (1977) 3079.
[16] A.D. Adler, F.R. Longo, J.D. Finarelli, J. Goldmacher, J. Assour, L. Korsakoff, J. Org. Chem. 32 (1967) 476.
[17] S.J. Narayanan, S. Venkatraman, S.R. Dey, B. Sridevi, V.R.G. Anand, T.K. Chandrashekar, Synlett 12 (2000) 1834.
[18] S. Venkatraman, V. Prabhuraja, R. Mishra, R. Kumar, T.K. Chandrashekar, W. Teng, K.R. Senge, Indian J. Chem. 42A (2003) 2191.
[19] J.S. Lindsey, I.C. Schreiman, H.C. Hsu, P.C. Kearney, A.M. Marguerettaz, J. Org. Chem. 52 (1987) 827.
[20] J.S. Lindsey, H.C. Hsu, I.C. Schreiman, Tetrahedron Lett. 41 (1986) 4969.
[21] V.A. Nadtochenko, N.N. Denisov, V.Y. Gak, N.V. Abramova, N.M. Loim, Russ. Chem. Bull. 48 (1999) 1900.
[22] V.A. Nadtochenko, D.V. Khudyakov, E.V. Vorontsov, N.M. Loim, F.E. Gostev, D.G. Tovbin, A.A. Titov, O.M. Sarkisov, Russ. Chem. Bull. 51 (2002) 986.
[23] V.N. Nemykin, M. McGinn, A.Y. Koposov, I.N. Tretyakova, E.V. Polshin, N.M. Loim, N.V. Abramova, Ukrainian Chem. J. 71 (2005) 79.
[24] V.N. Nemykin, C.D. Barrett, R.G. Hadt, R.I. Subbotin, A.Y. Maximov, E.V. Polshin, A.Y. Koposov, Dalton Trans. 31 (2007) 3378.
[25] N.M. Loim, N.V. Abramova, R.Z. Khaliullin, V.I. Sokolov, Russ. Chem. Bull. 46 (1997) 1193.
[26] C.H. Devillers, Recepteurs et materiaux rédox-actifs pour l'activation et la signalisation d'interactions moléculaires, PhD thesis, Université Joseph Fourier, Grenoble, 2006 (CCDC number for **1**Zn: 659850).
[27] A. Auger, A.J. Muller, J.C. Swarts, Dalton Trans. 33 (2007) 3623.
[28] N.M. Loim, N.V. Abramova, R.Z. Khaliullin, Y.S. Lukashov, E.V. Vorontsov, V.I. Sokolov, Russ. Chem. Bull. 47 (1998) 1016.
[29] D.T. Gryko, F. Zhao, A.A. Yasseri, K.M. Roth, D.F. Bocian, W.G. Kuhr, J.S. Lindsey, J. Org. Chem. 65 (2000) 7356.
[30] A. Auger, J.C. Swarts, Organometallics 26 (2007) 102.
[31] M. Kubo, Y. Mori, M. Otani, M. Murakami, Y. Ishibashi, M. Yasuda, K. Hosomizu, H. Miyasaka, H. Imahori, S. Nakashima, J. Phys. Chem. A 111 (2007) 5136.
[32] M. Kubo, M. Yukie, O. Masana, M. Masataka, I. Yukihide, Y. Masakazu, H. Kohei, M. Hiroshi, I. Hiroshi, N. Satoru, Chem. Phys. Lett. 429 (2006) 91.
[33] P.D.W. Boyd, A.K. Burrell, W.M. Campbell, P.A. Cocks, K.C. Gordon, G.B. Jameson, D.L. Officer, Z. Zhao, Chem. Commun. (1999) 637.
[34] S.W. Rhee, Y.H. Na, Y. Do, J. Kim, Inorg. Chim. Acta 309 (2000) 49.
[35] S.W. Rhee, B.B. Park, Y. Do, J. Kim, Polyhedron 19 (2000) 1961.
[36] J. Kim, S.W. Rhee, Y.H. Na, K.P. Lee, Y. Do, S.C. Jeoung, Bull. Korean Chem. Soc. 22 (2001) 1316.
[37] C.J. Medforth, in: K.S.K.M. Kadish, R. Guilard (Eds.), The Porphyrin Handbook, vol. 5, Academic Press, San Diego, 2000, pp 1.
[38] B. Koszarna, H. Butenschön, D.T. Gryko, Org. Biomol. Chem. 3 (2005) 2640.
[39] D.T. Gryko, J. Piechowska, J.S. Jaworski, M. Gałęzowski, M. Tasior, M. Cembor, H. Butenschön, New J. Chem. 31 (2007) 1613.
[40] O. Shoji, S. Okada, A. Satake, Y. Kobuke, J. Am. Chem. Soc. 127 (2005) 2201.
[41] O. Shoji, H. Tanaka, T. Kawai, Y. Kobuke, J. Am. Chem. Soc. 127 (2005) 8598.
[42] D. Kalita, M. Morisue, Y. Kobuke, New J. Chem. 30 (2006) 77.
[43] M. Morisue, D. Kalita, N. Haruta, Y. Kobuke, Chem. Commun. (2007) 2348.
[44] G.G.A. Balavoine, G. Doisneau, T. Fillebeen-Khan, J. Organomet. Chem. 412 (1991) 381.
[45] C. Bucher, C.H. Devillers, J.-C. Moutet, G. Royal, E. Saint-Aman, Chem. Commun. (2003) 888.
[46] C. Bucher, C.H. Devillers, J.-C. Moutet, G. Royal, E. Saint-Aman, New J. Chem. 28 (2004) 1584.
[47] E.S. Schmidt, T.S. Calderwood, T.C. Bruice, Inorg. Chem. 25 (1986) 3718.
[48] F. D'Souza, P.M. Smith, S. Gadde, A.L. McCarty, M.J. Kullman, M.E. Zandler, M. Itou, Y. Araki, O. Ito, J. Phys. Chem. B 108 (2004) 11333.
[49] L. Wei, K. Padmaja, W.J. Youngblood, A.B. Lysenko, J.S. Lindsey, D.F. Bocian, J. Org. Chem. 69 (2004) 1461.
[50] R.S. Loewe, A. Ambroise, K. Muthukumaran, K. Padmaja, A.B. Lysenko, G. Mathur, Q. Li, D.F. Bocian, V. Misra, J.S. Lindsey, J. Org. Chem. 69 (2004) 1453.
[51] A. Ambroise, R.W. Wagner, P.D. Rao, J.A. Riggs, P. Hascoat, J.R. Diers, J. Seth, R.K. Lammi, D.F. Bocian, D. Holten, J.S. Lindsey, Chem. Mater. 13 (2001) 1023.
[52] K.-L. Cheng, H.-W. Li, D.K.P. Ng, J. Organomet. Chem. 689 (2004) 1593.
[53] K.-W. Poon, W. Liu, P.-K. Chan, Q. Yang, T.-W.D. Chan, T.C.W. Mak, D.K.P. Ng, J. Org. Chem. 66 (2001) 1553.
[54] M.U. Winters, E. Dahlstedt, H.E. Blades, C.J. Wilson, M.J. Frampton, H.L. Anderson, B. Albinsson, J. Am. Chem. Soc. 129 (2007) 4291.
[55] R. Giasson, E.J. Lee, X. Zbao, M.S. Wrighton, J. Phys. Chem. 97 (1993) 2596.
[56] G. Vaijayanthimala, F. D'Souza, V. Krishnan, J. Coord. Chem. 21 (1990) 333.
[57] A.N. Cammidge, P.J. Scaife, G. Berber, L.H. David, Org. Lett. 7 (2005) 3413.
[58] T. Muraoka, K. Kinbara, T. Aida, Nature 440 (2006) 512.
[59] P.D. Beer, S.S. Kurek, J. Organomet. Chem. 336 (1987) C17.
[60] P.D. Beer, S.S. Kurek, J. Organomet. Chem. 366 (1989) C6.
[61] R.W. Wagner, P.A. Brown, T.E. Johnson, J.S. Lindsey, Chem. Commun. (1991) 1463.
[62] R.W. Wagner, T.E. Johnson, J.S. Lindsey, Tetrahedron 53 (1997) 6755.
[63] F. D'Souza, O. Ito, Coord. Chem. Rev. 249 (2005) 1410.
[64] D.M. Guldi, H. Imahori, J. Porphyrins Phthalocyanines 8 (2004) 976.
[65] M. Fujitsuka, O. Ito, H. Imahori, K. Yamada, H. Yamada, Y. Sakata, Chem. Lett. 28 (1999) 721.
[66] H. Imahori, H. Yamada, S. Ozawa, K. Ushida, Y. Sakata, Chem. Commun. (1999) 1165.
[67] H. Imahori, H. Yamada, Y. Nishimura, I. Yamazaki, Y. Sakata, J. Phys. Chem. B 104 (2000) 2099.
[68] H. Imahori, K. Tamaki, H. Yamada, K. Yamada, Y. Sakata, Y. Nishimura, I. Yamazaki, M. Fujitsuka, O. Ito, Carbon 38 (2000) 1599.
[69] H. Imahori, K. Tamaki, D.M. Guldi, C. Luo, M. Fujitsuka, O. Ito, Y. Sakata, S. Fukuzumi, J. Am. Chem. Soc. 123 (2001) 2607.
[70] S. Fukuzumi, H. Imahori, H. Yamada, M.E. El-Khouly, M. Fujitsuka, O. Ito, D.M. Guldi, J. Am. Chem. Soc. 123 (2001) 2571.
[71] H. Imahori, K. Tamaki, Y. Araki, Y. Sekiguchi, O. Ito, Y. Sakata, S. Fukuzumi, J. Am. Chem. Soc. 124 (2002) 5165.
[72] H. Imahori, M. Kimura, K. Hosomizu, T. Sato, T.K. Ahn, S.K. Kim, D. Kim, Y. Nishimura, I. Yamazaki, Y. Araki, O. Ito, S. Fukuzumi, Chem. Eur. J. 10 (2004) 5111.

[73] H. Imahori, Y. Sekiguchi, Y. Kashiwagi, T. Sato, Y. Araki, O. Ito, H. Yamada, S. Fukuzumi, Chem. Eur. J. 10 (2004) 3184.
[74] F. D'Souza, R. Chitta, S. Gadde, D.-M. Shafiqul Islam, A.L. Schumacher, M.E. Zandler, Y. Araki, O. Ito, J. Phys. Chem. B 110 (2006) 25240.
[75] F. Fungo, L.A. Otero, L. Sereno, J.J. Silber, E.N. Durantini, J. Mater. Chem. 10 (2000) 645.
[76] H. Imahori, D.M. Guldi, K. Tamaki, Y. Yoshida, C. Luo, Y. Sakata, S. Fukuzumi, J. Am. Chem. Soc. 123 (2001) 6617.
[77] D.M. Guldi, H. Imahori, K. Tamaki, Y. Kashiwagi, H. Yamada, Y. Sakata, S. Fukuzumi, J. Phys. Chem. A 108 (2004) 541.
[78] Y. Li, Z. Gan, N. Wang, X. He, Y. Li, S. Wang, H. Liu, Y. Araki, O. Ito, D. Zhu, Tetrahedron 62 (2006) 4285.
[79] H. Nakagawa, K. Ogawa, A. Satake, Y. Kobuke, Chem. Commun. (2006) 1560.
[80] K. Uosaki, T. Kondo, X.-Q. Zhang, M. Yanagida, J. Am. Chem. Soc. 119 (1997) 8367.
[81] M. Yanagida, T. Kanai, X.-Q. Zhang, T. Kondo, K. Uosaki, Bull. Chem. Soc. Jpn. 71 (1998) 2555.
[82] N.B. Thornton, H. Wojtowicz, T. Netzel, D.W. Dixon, J. Phys. Chem. B 102 (1998) 2101.
[83] T. Kondo, T. Kanai, K. Iso-o, K. Uosaki, Z. Phys. Chem. 212 (1999) 23.
[84] J. Tanihara, K. Ogawa, Y. Kobuke, J. Photochem. Photobiol. A 178 (2006) 140.
[85] P.D. Beer, M.G.B. Drew, R. Jagessar, J. Chem. Soc., Dalton Trans. (1997) 881.
[86] M. Hisatome, S.-I. Takano, K. Yamakawa, Tetrahedron Lett. 26 (1985) 2347.
[87] M.C. Hodgson, A.K. Burrell, P.D.W. Boyd, P.J. Brothers, C.E.F. Rickard, J. Porphyrins Phthalocyanines 6 (2002) 737.
[88] F. D'Souza, M.E. El-Khouly, S. Gadde, M.E. Zandler, A.L. McCarty, Y. Araki, O. Ito, Tetrahedron 62 (2006) 1967.
[89] P.D.W. Boyd, A. Hosseini, Acta Crystallogr., Sect. C: Cryst. Struct. Commun. E 62 (2006) 1542.
[90] T.-A. Okamura, T. Iwamura, H. Yamamoto, N. Ueyama, J. Organomet. Chem. 692 (2007) 248.
[91] J.E. Maskasky, M.E. Kenney, J. Am. Chem. Soc. 93 (1971) 2060.
[92] K.M. Kadish, Q.Y. Xu, J.M. Barbe, Inorg. Chem. 26 (1987) 2566.
[93] Q.Y. Xu, J.-M. Barbe, K.M. Kadish, Inorg. Chem. 27 (1988) 2373.
[94] G.B. Maiya, J.M. Barbe, K.M. Kadish, Inorg. Chem. 28 (1989) 2524.
[95] L.M. Scolaro, M.R. Plutino, A. Romeo, R. Romeo, G. Ricciardi, S. Belvisoc, A. Albinatid, Dalton Trans. (2006) 2551.
[96] M. Schmittel, R.S.K. Kishorea, J.W. Bats, Org. Biomol. Chem. 5 (2007) 78.
[97] P. Tecilla, R.P. Dixon, G. Slobodkin, D.S. Alavi, D.H. Waldeck, A.D. Hamilton, J. Am. Chem. Soc. 112 (1990) 9408.
[98] A.K. Burrell, W. Campbell, D.L. Officer, Tetrahedron Lett. 38 (1997) 1249.
[99] A.K. Burrell, W.M. Campbell, D.L. Officer, S.M. Scott, K.C. Gordon, M.R. McDonald, J. Chem. Soc., Dalton Trans. (1999) 3349.
[100] L. Jiao, B.H. Courtney, F.R. Fronczek, K.M. Smith, Tetrahedron Lett. 47 (2006) 501.
[101] S. Venkatraman, R.K. Kumar, J. Sankar, T.K. Chandrashekar, K. Sendhil, C. Vijayan, A. Kelling, M.O. Senge, Chem. Eur. J. 10 (2004) 1423.
[102] R. Kumar, R. Misra, V. Prabhuraja, T.K. Chandrashekar, Chem. Eur. J. 11 (2005) 5695.
[103] L. Jixiang, Z. Qingfu, X. Huijun, Chin. Chem. Lett. 4 (1993) 339.
[104] Z. Jin, K. Nolan, C.R. McArthur, A.B.P. Lever, C.C. Leznoff, J. Organomet. Chem. 468 (1994) 205.
[105] F.T. Baumann, M.S. Nasir, J.W. Sibert, A.J.P.O. White, M.M.D.J. Williams, A.G.M. Barrett, B.M. Hoffman, J. Am. Chem. Soc. 118 (1996) 10479.
[106] J. Silver, J.L. Sanchez, C.S. Frampton, Inorg. Chem. 37 (1998) 411.
[107] K.-W. Poon, Y. Yan, X.-Y. Li, D.K.P. Ng, Organometallics 18 (1999) 3528.
[108] A. González, P. Vázquez, T. Torres, Tetrahedron Lett. 40 (1999) 3263.
[109] A. González-Cabello, P. Vázquez, T. Torres, J. Organomet. Chem. 637–639 (2001) 751.
[110] V.N. Nemykin, N. Kobayashi, Chem. Commun. (2001) 165.
[111] N. Chabert-Couchouron, C. Reibel, C. Marzin, G. Tarrago, An. Quim. Int. Ed. 92 (1996) 70.
[112] N. Chabert-Couchouron, C. Marzin, G. Tarrago, New J. Chem. 21 (1997) 355.
[113] N. Chabert-Couchouron, C. Marzin, C. Reibel, G. Tarrago, New J. Chem. 21 (1997) 993.
[114] C. Bucher, C.H. Devillers, J.-C. Moutet, J. Pécaut, G. Royal, E. Saint-Aman, F. Thomas, Dalton Trans. 22 (2005) 3620.
[115] J.L. Sessler, R.S. Zimmerman, C. Bucher, V. Král, B. Andrioletti, Pure Appl. Chem. 73 (2001) 1041.
[116] P.A. Gale, J.L. Sessler, V. Král, Chem. Commun. (1998) 1.
[117] M. Bernátková, H. Dvořáková, B. Andrioletti, V. Král, P. Bouř, J. Phys. Chem. A 109 (2005) 5518.